

8-8-2015

## Electrochemical Characterization of Self-Assembled Monolayers on Gold Substrates Derived from Thermal Decomposition of Monolayer-Protected Cluster Films

Michael C. Leopold  
*University of Richmond*, mleopold@richmond.edu

Tran T. Doan

Melissa J. Mullaney

Andrew F. Loftus

Christopher M. Kidd

Follow this and additional works at: <https://scholarship.richmond.edu/chemistry-faculty-publications>

 Part of the [Inorganic Chemistry Commons](#)

This is a pre-publication author manuscript of the final, published article.

---

### Recommended Citation

M.C. Leopold, T.T. Doan, M.J. Mullaney, D.J. Tognarelli, A.F. Loftus, and C.M. Kidd, "Electrochemical Characterization of Self-Assembled Monolayers on Gold Substrates Derived from Thermal Decomposition of Monolayer-Protected Cluster Films," *Journal of Applied Electrochemistry* 2015, 45(10), 1069-1084.

This Post-print Article is brought to you for free and open access by the Chemistry at UR Scholarship Repository. It has been accepted for inclusion in Chemistry Faculty Publications by an authorized administrator of UR Scholarship Repository. For more information, please contact [scholarshiprepository@richmond.edu](mailto:scholarshiprepository@richmond.edu).

*For submission to J. of Applied Electrochemistry*

**Electrochemical Characterization of Self-Assembled Monolayers on Gold Substrates  
Derived from Thermal Decomposition of Monolayer-Protected Cluster Films**

Michael C. Leopold,\* Tran T. Doan, Melissa J. Mullaney, Andrew F. Loftus,  
and Christopher M. Kidd

*Department of Chemistry, Gottwald Center for the Sciences, University of Richmond  
Richmond, VA 23173*

**Abstract**

Networked films of monolayer protected clusters (MPCs), alkanethiolate stabilized gold nanoparticles, can be thermally decomposed to form stable gold on glass substrates that are subsequently modified with self-assembled monolayers (SAMs) for use as modified electrodes. Electrochemical assessment of these SAM modified gold substrates, including double-layer capacitance measurements, linear sweep desorption of the alkanethiolates, and diffusional redox probing, all show that SAMs formed on gold supports formed from thermolysis of MPC films possess substantially higher defect density compared to SAMs formed on traditional evaporated gold. The density of defects in the SAMs on thermolyzed gold is directly related to the strategies used to assemble the MPC film prior to thermolysis. Specifically, gold substrates formed from thermally decomposing MPC films formed with electrostatic bridges between carboxylic acid modified MPCs and metal ion linkers are particularly sensitive to the degree of metal exposure during the assembly process. While specific metal dependence was observed, metal concentration within the MPC precursor film was determined to be a more significant factor. Specific MPC film linking strategies and pretreatment methods that emphasized lower metal exposure resulted in gold films that supported SAMs of lower defect density. The defect density of a SAM-modified electrode is shown to be critical in certain electrochemical experiments such as protein monolayer electrochemistry of adsorbed cytochrome c. While the thermal decomposition of nanoparticle film assemblies remains a viable and interesting technique for coating both flat and irregular shaped substrates, this study provides electrochemical assessment tools and tactics for determining and controlling SAM defect density on this type of gold structure, a property critical to their effective use in subsequent electrochemical applications.

---

**Keywords:** self-assembled monolayer, monolayer protected clusters, nanoparticle films, double-layer capacitance, linear sweep desorption, redox probe voltammetry, thin gold films

\*To whom correspondence should be addressed. Email: [mleopold@richmond.edu](mailto:mleopold@richmond.edu). Phone: (804) 287-6329. Fax: (804) 287-1897

## 1. Introduction

Stabilized forms of metallic nanoparticles (NPs) can be arranged into higher order assemblies that are of interest because of their unique optical, electrochemical, and structural properties and their potential use in macroscopic applications as materials coatings. Assemblies of NPs have been investigated as functional materials for a variety of specific uses, including potential bio-interfaces [1, 2], fundamental electron transfer systems [3], analytical sensors [4], and chromatography media [5-8], for example. Monolayer protected clusters (MPCs) represent an important and highly versatile example of ligand-stabilized metallic nanomaterials explored in these capacities [9, 10]. MPCs offer a high level of structural stability and are easily functionalized, making them ideal for incorporation into a film with a multitude of interparticle linking mechanisms. Various types of MPC films have been exploited as sensing materials, most notably for chemical vapor [11-15] and metal ion detection [16].

One unique application of interest is the use of assembled NP films as a precursor to thin metal film deposition [17-22]. Thin metal layers, especially those composed of coinage metals, are of particular interest for a range of applications, including modified electrodes [23], computer media [24], electronics [25], and protective films [26]. Several groups have explored thin metal films derived from NP film assemblies [17-22]. Typically, NP films have been assembled on a substrate and subsequently decomposed to create a metallic coating. Natan and coworkers formed multi-layer films of citrate-stabilized NPs (Au, Ag, Au/Ag alloy) with various sized cross-linking molecules. As these films were grown thicker, those formed with shorter linking ligands, e.g., 2-mercaptoethylamine, were observed to coalesce into bulk metal coatings [18]. Thin gold films were created by Claus et al. by thermally treating dithiol-linked MPC assemblies [19]. In similar work by Nagasawa, silver metallation of a surface was achieved by thermally

decomposing stearate-coated NPs [20]. In all cases, thermal heating was kept below the melting point of the NP's bulk metal and was instead used as a means of disengaging the linking mechanism within the MPC film assembly and subsequently removing the NP's protecting ligands.

Due to their superior stability and high versatility, alkanethiolate-based MPCs have also been assembled into films and explored as precursors to thin metal coatings. Colvin's laboratory attached MPCs of this nature to modified colloidal silica followed by thermal treatment by a propane torch at 575°C to produce freestanding, macroporous metal films [21]. Using slightly lower thermolysis temperatures (<400°C), Zhong and coworkers characterized metal films derived from MPC assemblies linked with both covalent (dithiol) and hydrogen bonding interparticle interactions. Spectroscopic characterization of the systems suggested that the structure of the resulting metal film was highly influenced by the linking mechanisms employed to create the MPC film precursor [22].

Murray and coworkers investigated the formation of thin metal layers resulting from the modest thermal treatment (<300°C) of MPC films either drop-cast from solution or assembled via electrostatic bridges between carboxylic acid functionalized MPCs and copper ions on a glass slide [17]. After thermolysis, the resulting thin gold film formed from drop-cast material lacked adhesion to the underlying glass substrate while stable, continuous gold films were readily formed from the electrostatically-linked MPC film assemblies. Murray's work succeeded in establishing methodology for effectively coating an irregularly shaped or three-dimensional surface with high quality, mechanically stable, thin metal films. Metal films formed in this manner were found to have physical properties similar to that of commercially available evaporated metal substrates [17]. Unlike traditional evaporated gold, usually available only in a

planar geometry, the use of nanoparticle films as a precursor for surface metallation allows for the application of thin metal films to an object of any size or shape that can be affixed with an MPC film and subsequently thermolyzed [17].

The reports described above all focus on the thermal deposition of a thin layer of metal onto a surface from a nanoparticle film precursor. From their work and others, it has been established that even modest thermal treatment of an MPC film composite results in the breakdown of interparticle linking followed by the liberation of the stabilizing ligands and the coalescence of metal directly onto the substrate surface. In the case of Murray's alkanethiolate MPCs, thermolysis results in the disintegration of carboxylic acid–metal ion–carboxylic acid linking bridges, subsequent liberation of disulfides, and the deposition of gold onto the substrate [17]. In all these reports, however, specific connections between how aspects of the NP (MPC) film assembly, prior to thermal decomposition, affect the properties and functionality, in terms of consequences for typical electrochemical applications of thin gold films (see below), were unexplored.

A primary use of thin metal films is as a platform for self-assembled monolayers (SAMs). For over 25 years, alkanethiol-based SAMs have seen an enormous amount of attention for a variety of purposes ranging from biosensor design to corrosion protection, with several excellent reviews available [27-29]. These self-assembling films, most commonly formed on gold substrates, provide a structurally stable and well-defined interface that can be tailored to exhibit specific chemical interactions by altering the end group and/or chainlength of its alkanethiol components. Several reports indicate that the order and structure of SAMs, including their defect density, is highly sensitive to the topography of the underlying gold substrate. From that work, it appears that this factor is heavily influenced by the type of gold and the

pretreatment applied to the gold prior to SAM modification [30-32]. Electrochemical techniques such as voltammetry have been shown to be an effective tool for assessing defect density and general structure of SAMs on gold substrates [33].

In this report, we present an intensive electrochemical analysis of  $\omega$ -substituted SAMs on gold substrates that were produced from the thermal treatment of MPC films. Multi-layer MPC films were assembled with different interparticle linking strategies and heat treated under moderate temperatures to produce thin gold films on glass substrates. These films were subsequently modified with SAMs of varying chainlength and terminal functionality before being thoroughly characterized with electrochemical techniques designed to assess the quality and integrity of the SAM adlayers on these uniquely formed surfaces. Particular attention was given to determining if the linking mechanism and/or method of assembly of the MPC films had an impact on the properties of the SAM formed on the thin gold film after thermolysis. Results were compared directly to those of SAMs on traditional evaporated gold substrates that are commercially available and commonly used in electrochemistry. This study expands upon previous work [17] establishing methods of translating NP assemblies into thin metal films by examining a specific application of the films, namely as a SAM support material in the context of protein monolayer electrochemistry [2]. Our results suggest that the quality of SAMs formed on the nanoparticle gold is highly dependent on the specific assembly of the MPC film precursor, a development that can have substantial effects on potential applications of SAMs.

## 2. Experimental Methods and Materials

### 2.1 Apparatus, instrumentation, and materials

Electrochemical measurements were carried out on CH Instruments Electrochemical Analyzers (Model 650A or 610B). Evaporated gold substrates were purchased from EMF Corporation (Ithaca, NY) and mounted as previously described [34], in house “sandwich” cells featuring Ag/AgCl (satr. KCl) reference electrodes (Microelectrodes, Inc.). UV-Vis spectroscopy was performed on a dual beam spectrophotometer (ThermoSpectronic-Unicam Model UV500) using a 3-MPTMS-modified glass slide as a reference. Unless otherwise specified, all chemicals used were available commercially and of analytical-reagent grade.

### 2.2. Procedures

#### 2.2.1. Glass slide preparation

Glass slides were prepared for MPC growth based on previously reported procedures [35-37]. Briefly, glass slides (Fisher-finest) were cut into 2.5 x 1.0 cm pieces and submerged in Piranha solution (2:1 ratio of concentrated H<sub>2</sub>SO<sub>4</sub> to 30 % H<sub>2</sub>O<sub>2</sub>) for 15 minutes. **WARNING:** *Piranha solution reacts violently with organic materials; use extreme caution when handling this material.* Slides were rinsed thoroughly with purified water (18 MΩ·cm) and propanol before immersion in a near boiling solution of propanol, water, and 3-mercaptopropyl trimethoxy silane (3-MPTMS, Aldrich) for 45 minutes [38]. After immersion in the silane, the slides were rinsed thoroughly with propanol, dried in a stream of nitrogen, and allowed to cure in an oven at 100° C for at least one hour. The entire silanization procedure was then repeated a second time before the slides were stored in the oven until further use.

### 2.2.1. Monolayer-protected cluster synthesis and functionalization

Hexanethiolate-coated MPCs were prepared as previously described using a modified Brust procedure [39]. Briefly, tetraoctylammonium bromide was used as a transfer reagent to move gold salt ( $\text{AuCl}_4^-$ ) from an aqueous phase to a toluene organic phase. Hexanethiol (Aldrich) was added to the organic phase in a 3:1 ratio of thiol-to-gold. Rapid addition of a strong reductant ( $\text{NaBH}_4$ ) and stirring overnight at  $0^\circ\text{C}$  resulted in a slurry of hexanethiolate ( $\text{C}_6$ ) protected nanoparticles that could then be rotary evaporated and collected on a glass frit with copious acetonitrile (ACN) washing to produce MPCs with an *average* composition of  $\text{Au}_{144}(\text{C}_6)_60$  [35-37]. To reduce the polydispersity of the product, “annealing” procedures described by Hicks et al. were employed [40] where the MPC material was re-dissolved in methylene chloride and stirred (24 hours) in the presence of additional hexanethiol (1:50 ratio of thiol-to-MPC). The annealed MPCs were again collected as described above and differential pulse voltammetry was used to observe slightly more defined quantized double layer charging, an indication of modestly improved polydispersity.

MPCs were functionalized for film growth using place-exchange reactions [41-42]. Briefly, MPCs and 11-mercaptoundecanoic acid (MUA) were co-dissolved in tetrahydrofuran and stirred for approximately 72 hours. The mixture was rotary evaporated, precipitated with anhydrous ACN, and recollected on a glass frit with several additional washings of ACN. NMR analysis of liberated disulfides upon iodine-induced decomposition of the MPCs in  $\text{CD}_2\text{Cl}_2$  was used to characterize the extent of functionalization (see Supplementary Materials). This procedure typically produced MPCs with an average composition of  $\text{Au}_{144}(\text{C}_6)_{32-37}(\text{MUA})_{23-28}$  as has been observed in other reports [11,17,35-37].



2.2.2. *MPC film assembly and thermal treatment*

Assembly procedures for electrostatic-linked (i.e. metal ion – carboxylic acid bridged) films were adopted from literature reports [35-37]. Briefly, solutions of a metal salt, e.g., 0.1 M copper perchlorate or 0.2 M zinc nitrate[44], and MPC (1 mg/1 mL) in ethanol were prepared. The silanized slide was subjected to sequential “dipping cycles” consisting of immersing it for 1 hour in the metal ion solution followed by thorough ethanol rinsing (continuously for 2-3 minutes) and subsequent exposure to the MPC solution for another hour, followed by additional extensive rinsing with ethanol. Research in our lab and others has shown that this procedure, if continuously repeated, results in multilayer growth of an MPC film on the glass slide, observed as a thick, black coating [11,17,35-37]. Growth progress was monitored via UV-Vis spectroscopy as a reasonable determination of general thickness (see **Scheme I**, Step (1), MPC film assembly and UV-Vis tracking). Film growth was continued until an absorbance at 300 nm of  $\geq$  approximately 3.0 a.u. was achieved, a process usually requiring between 7 and 10 dipping cycles (**Scheme I**). Based on estimations from Murray’s work [17], this absorbance corresponds roughly to a film consisting of approximately 300-400 monolayers of MPC and an average film thickness of almost 1  $\mu\text{m}$  on each side of the glass slide, a visibly thick black coating (Supplementary Materials). We note here that films grown to greater thicknesses did not yield significantly different results than described in this report (results not included).

After MPC films were grown to the targeted thickness, they were subsequently thermolyzed in a vented oven at 375° C for 15-20 minutes as described in the literature. Temperature was carefully controlled in order to not approach the softening temperature of gold, staying well below the melting transition temperature (1064°C [45]) as well [17]. Upon removal from the oven, the black assembly had transformed to a shiny, mirror-like, gold coating on the

glass slide (Supplementary Materials). These gold films have previously been characterized and determined to be comparable to evaporated gold substrates [17]. Prior to use in this study, we found that gold coatings formed in this manner are mechanically stable by the Crook's "tape test", exhibiting excellent adhesion to the glass [43]. As described in the literature, the bulk loss of the organic component of the film reduces the thickness an order of magnitude, estimated conservatively as being over 100 Å thick [17]. For this study, the slides were allowed to cool for several minutes and then immediately modified with a self-assembled monolayer (SAM) as described below. Commercially purchased evaporated gold substrates were electrochemically cleaned as previously shown with cyclic voltammetry in 0.1 M H<sub>2</sub>SO<sub>4</sub> and 0.01 M KCl prior to SAM modification [34].

### *2.2.3. SAM Modification of Gold Substrates and Electrochemical Cell Loading*

The thermolyzed nanoparticle-based gold as well as the purchased evaporated gold substrates were immersed for 48 hours in one of the following 5 mM alkanethiol solutions (Aldrich): butane thiol (BT), octane thiol (OT), dodecane thiol (DDT), 6-mercaptohexanoic acid (MHA) [46], 11-mercaptoundecanoic acid (MUA), 16-mercaptohexadecanoic acid (MHDA), 6-mercaptohexanol (MHOL), or 11-mercaptoundecanol (MUD). After initial SAM modification, the substrates were rinsed thoroughly with ethanol and mounted in the sandwich cells. To compensate for any damage to the SAM during handling, additional 5 mM alkanethiol solution was added to the cell for another 48 hours and then thoroughly rinsed with ethanol and water before the SAM was characterized using electrochemical-based techniques.

## **3. Theory – Electrochemical SAM Characterization**

### 3.1. Double Layer Capacitance of SAM-modified Electrodes

Double layer capacitance ( $C_{dl}$ ) measurements are based in theory on the Helmholtz model for the electrical double layer of an electrode in solution. The Helmholtz theory essentially treats the electrode-solution interface as an ideal capacitor where the planes of charge, located at the electrode surface and at the closest ionic charge from solution compensating the charge on the electrode, are separated by a dielectric layer. According to this model,  $C_{dl}$  usually adheres to the following relationship:

$$C_{dl} \approx \frac{\epsilon \cdot \epsilon_0}{d} \quad (1)$$

where  $\epsilon$  is the dielectric constant, an indicator of the polarizability of the separating medium,  $d$  is the distance between the planes of charge, and  $\epsilon_0$  is the permittivity of free space constant [47]. It follows that a SAM adlayer, composed of unfunctionalized alkanethiolates, would result in a substantially lower value of  $C_{dl}$  compared to a bare metal electrode because of both an increase in  $d$  and a decrease in  $\epsilon$ . As the chainlength of the alkanethiols used to make the SAM increases, capacitance is observed to decrease. Due to a substantial increase of lateral interactions among the methylene backbones of components of a SAM, films formed from longer chain alkanethiols (i.e., greater number of methylene units) are known to exhibit a greater degree of order compared to shorter chain films [33]. Thus, these films are better able to exclude water and other polar species, lowering the dielectric of the capacitor and decreasing  $C_{dl}$ . Likewise, more polar end groups systematically increase the polarizability of the dielectric layer, making SAMs formed from  $\omega$ -substituted alkanethiol exhibit higher  $C_{dl}$ . Of note for this study is that  $C_{dl}$  also increases with the presence of defects in the SAM, a factor affecting both the average distance and dielectric [48]. Thus,  $C_{dl}$  measurements can be used as a tool to assess defect density in SAMs.

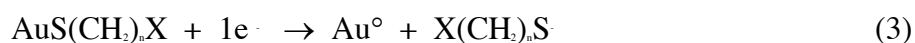
For simple systems such as SAMs on gold,  $C_{dl}$  is easily measured by immersing the SAM in a solution of supporting electrolyte and performing cyclic voltammetry. In the absence of a redox species in solution (Faradaic current), only non-Faradaic or charging current is recorded. For the potential windows scanned in these experiments, the current at 250 mV vs. the Ag/AgCl reference electrode was recorded. Based on the equation below, this current can be translated into  $C_{dl}$ :

$$C_{dl} (\mu\text{F}/\text{cm}^2) = \frac{|i|}{2 \cdot \nu \cdot A \times 10^{-6}} \quad (2)$$

where  $i$  is the total current (amps),  $\nu$  is the scan rate (V/sec), and  $A$  is the area of the working electrode ( $\text{cm}^2$ ).

### 3.2. Linear Sweep Voltammetric Desorption of SAMs

The application of linear voltage sweep toward increasingly negative potentials to a SAM under basic solution conditions results in the reductive desorption of the thiolated adlayer according to the following reaction:



which produces a sharp, cathodic wave in the voltammogram [51]. The area of this peak has been used in previous reports as a means of determining the surface concentration of thiolates [52]. Reductive desorption can also be useful in assessing the relative integrity of SAMs as well. The potential at which the reductive wave is observed is highly dependent on several factors including the strength of the Au-S bond as well as lateral interactions among the SAM components (i.e., intermolecular interactions between endgroups and alkyl chains). Thus, SAMs comprised of longer chainlength alkanethiolates will require more negative potentials for electrochemically-induced desorption [33]. Since the reductive desorption process requires at

least partial solvent access to the electrode surface, a SAM with high defect density will be reduced at a much lower negative potential than the same film without defects. Often, linear sweep voltammetry used for this purpose results in multiple cathodic peaks at negative potentials, typical of alkanethiolate desorption from a polycrystalline gold surfaces such as those used in our study. Since our main concern was a qualitative comparison of SAM defect density, we measured the peak potential of the first reductive wave as an initial indicator that SAM integrity had been compromised.

### *3.3. Redox Probe Voltammetry at SAM-modified Electrodes*

A classical property of a well-formed SAM is its ability to inhibit Faradaic electron transfer (ET) of solution redox species [33]. The oxidation and reduction of a redox species in solution is dependent on its access to the electrode surface. Alkanethiol SAMs of sufficient blocking ability can prevent the facile approach of most aqueous redox species as it is energetically unfavorable for a hydrophilic molecule to traverse a well-packed hydrocarbon layer. Cyclic voltammetry of a redox couple in solution at a SAM-modified electrode indicates blocking behavior by the attenuation or loss of the voltammetric waves during potential sweeps. Moreover, SAMs can cause a redox couple to display more irreversible peaks (i.e., a greater separation of anodic and cathodic peak potentials,  $\Delta E_p$  or  $|E_{p,c} - E_{p,a}|$ ) as a manifestation of effective blocking ability. For SAMs having higher defect density, solution redox molecules gain access to the electrode via pinhole defects. At a SAM with a high density of pinholes, the voltammetry of the molecule in solution often referred to as a redox probe, will resemble that of the probe at a bare metal electrode in terms of size, shape, and ET kinetics. Thus, recording the cyclic voltammetry of redox probes at various types of SAMs is a common and effective way of

learning about the density of defects in films. Some common redox probes, which can vary in their sensitivity for defects, include metal ion couples [53], ruthenium hexamine chloride ( $\text{Ru}(\text{NH}_3)_6\text{Cl}_2$ ) [54], potassium ferricyanide ( $\text{K}_3\text{Fe}(\text{CN})_6$ ) [55], ferrocene (Fc) and Fc derivatives [56].

#### 4. Results and Discussion

The thermal treatment of assembled MPC films is an established method for creating novel thin films of gold. One application of gold substrates is as a support for multi-purpose SAMs. To the best of our knowledge, the important properties of SAMs formed on gold substrates created in this manner have not been characterized. Electrochemistry, namely voltammetry, is a relatively easy and effective methodology for characterizing SAM adlayers, especially in the determination of film defect density. The following results were collected during electrochemical testing of SAMs varying in end group and chainlength, at gold substrates formed from thermal treatment of networked MPC films (MPC gold), and at evaporated gold substrates, for comparison.

##### *4.1. SAMs on Gold from Thermolyzed Metal-Linked MPC Film Assemblies*

Carboxylic acid-modified MPCs linked via carboxylic acid-metal ion (II)-carboxylic acid interparticle bridges were assembled into film geometries on a glass slides until an absorbance of 3.0 a.u. or greater at 300 nm was achieved (**Scheme I**). These films were formed and subsequently thermolyzed in an oven to produce a shiny gold adlayer that was immediately modified with a specific SAM (see Section 2.2.2. for details). These SAMs, in parallel with identical SAMs on evaporated gold, were then characterized with electrochemical experiments

including double layer capacitance measurements, linear sweep voltammetric desorption of the SAMs, and voltammetry of solution based redox probe molecules at the SAM – all experiments designed to assess the quality (i.e., defect density) of the thin film adlayers.

#### 4.1.1. Double Layer Capacitance Results

One of the simplest methods of assessing the quality of a SAM at a metal electrode is to measure the double layer capacitance ( $C_{dl}$ ) of the system, a parameter directly proportional to the non-Faradaic charging current during simple cyclic voltammetry (see Section 3.1.) in only supporting electrolyte solution. For example, the inset of **Figure 1** shows voltammetric measurements of  $C_{dl}$  in 1.0 M KCl on evaporated gold substrates modified with methyl terminated SAMs of increasing chainlength (BT < OT < DDT). As expected, the charging current, measured at 250 mV and depicted by the thickness of the voltammograms, drastically decreases, along with the corresponding calculated  $C_{dl}$ , as the SAM structure becomes more structurally ordered with longer chainlength alkanethiol components.

In similar experiments, **Figure 1** also compares the  $C_{dl}$  of DDT SAMs on evaporated gold to DDT SAMs on gold formed from thermolyzed metal-linked (M-L) MPC films constructed on glass slides with both  $Zn^{2+}$  and  $Cu^{2+}$  linkages. As seen by the results, the SAMs formed on the gold substrates formed from thermolyzed NP films display strikingly higher charging currents and subsequently have much larger  $C_{dl}$  values than their counterparts on evaporated gold. Likewise,  $C_{dl}$  measurements for SAMs with varying end groups and chainlengths, including long and short chain hydroxyl and carboxylic acid terminated films formed on the different types of gold substrates are displayed graphically in **Figure 2** and summarized along with the other results in **Table 1** with estimates of the uncertainty associated with the measurements. In the

interest of simplifying the graphical and tabular representation of our results throughout our report, we have sometimes omitted the results for SAMs formed on thermolyzed MPC films assembled with  $Zn^{2+}$  metal linkers during the initial comparisons because of the data's similarity to the results observed with  $Cu^{2+}$  linked films. The minor metal dependence observed in these materials is discussed in a later section. For comparison purposes, the data for  $Zn^{2+}$  M-L MPC films is included in tables found in the Supplementary Materials.

Collectively, the results of Figure 2 and Table 1 yield some notable trends. In addition to having significantly smaller  $C_{ad}$ , all the SAMs on evaporated gold substrates (Figure 2, closed symbols and inset) adhere to the expected trend regarding chainlength - decreasing  $C_{ad}$  with increasing number of methylene units or total carbons. Likewise, the expected endgroup effect, with more polar endgroups yielding higher  $C_{ad}$  values in the following order:  $COOH > OH > CH_3$ , is also clearly observed [33] with SAMs on evaporated gold. Interestingly, both the chainlength and functional group trends are also evident with identical SAMs formed on the gold formed from M-L MPC films (Figure 2, open symbols), though their actual  $C_{ad}$  values are 1-2 orders of magnitude greater. The one exception to the expected functional group trend for SAMs is that of the hydroxyl terminated SAMs on the M-L substrates was unexpectedly lower than that of methyl terminated films on these surfaces ( $COOH > CH_3 > OH$ ). This finding, however, is not totally unprecedented as Miller et al. observed hydroxyl terminated SAMs to have lower  $C_{ad}$  than their equivalent alkanethiol SAMs, a result attributed to hydrogen bonding stabilization of the hydroxyl groups [49]. Also noteworthy in the comparison of the data is the higher degrees of uncertainty associated with the  $C_{ad}$  of SAMs formed on the substrates derived from MPC films. Higher uncertainty is often observed with shorter chain SAMs and is a reflection of the higher level of disorder inherent in these films [33]. In the case of the thermolyzed M-L MPC



substrates, the film-to-film variation seemed to persist through all chainlengths tested. One explanation of this high uncertainty with SAMs at gold derived from the NP films is an inherent variation in film-to-film quality due to the numerous steps they require and the increased handling required by the preparation procedures for these substrates.

Of particular note in these results is the striking difference between the measured  $C_{dl}$  of SAMs on the two types of substrates. For every SAM tested, the  $C_{dl}$  of the SAM on M-L MPC gold substrates was at least one order of magnitude higher than the same film on evaporated gold. These results suggest a systematic difference between the two film systems, most likely the result of a significantly greater density of defects in the thermolyzed NP gold films. The same trends were observed regardless of how thick the MPC films were grown prior to thermal treatment (results not shown). A greater degree of defect density would result in a breakdown of the dielectric layer and a subsequent increase in  $C_{dl}$  as seen here. Because SAMs are often utilized in bioanalytical applications [28,33], the  $C_{dl}$  of SAMs at these substrates was also measured in a second electrolyte, sodium phosphate buffer (Na-PB) at pH 7 and the same general trends seen with KCl were observed with Na-PB solutions (see Supplementary Materials for examples). The lower values of  $C_{dl}$  in Na-PB relative to KCl electrolyte are consistent with the hydration and permeability of ions into films of this nature [50].

#### 4.1.2. SAM Desorption Results

Linear sweep voltammetric desorption of the SAMs was employed as a supplemental method to see if the SAMs at the thermolyzed M-L gold films possessed a higher density of defects compared to SAMs at evaporated gold substrates. As described in Section 3.2, SAMs with higher defect density are expected to desorb at more positive potentials than less defective

films. **Figure 3A** shows linear sweep voltammograms of the reductive desorption of DDT SAMs from both the Cu<sup>2+</sup> M-L MPC gold and evaporated gold substrates. The peak potential ( $E_p$ ) for the evaporated gold-supported SAM is at much greater negative potential, indicating the superior structural integrity of this film compared to its counterpart on the Cu<sup>2+</sup> MPC gold. **Figure 3B** shows collective desorption results for methyl terminated SAMs of varying chainlength ( $n$ ) on evaporated gold (closed symbols) compared to the same films at thermolyzed Cu<sup>2+</sup> M-L MPC films (open symbols). Both substrates exhibit the expected chainlength trend with longer chainlength SAMs yielding more negative desorption peak potentials – an effect observed regardless of the endgroup. However, the reduction potential for SAMs on M-L Cu<sup>2+</sup> MPC gold were systematically less negative potentials than their corresponding films on evaporated gold. Cumulative desorption results for all the SAMs tested on the gold substrates are shown in **Table 2**. In all cases, the SAM formed on the Cu<sup>2+</sup> MPC gold was more easily desorbed (i.e. less negative cathodic peak potentials) than the same SAM formed on evaporated gold. These results, as with the  $C_{dl}$ , suggest that the SAMs formed on the NP gold have a higher defect density. Desorption results for SAMs at thermolyzed Zn<sup>2+</sup> M-L MPC films showed similar trends (Supplementary Materials).

#### 4.1.3. Redox Probing

As a final test for defect density in SAMs at these gold substrates, the voltammetry of a solution species or redox probe molecule at the SAM interface was investigated. The theory of using redox probe voltammetry to assess defects in SAMs was discussed in Section 3.3. Briefly, greater peak splitting in the cyclic voltammetry of the redox probes is indicative of SAMs with greater blocking capacity and a corresponding lower density of defects. For the SAM/Au

systems studied here, we first utilized the negatively charged potassium ferricyanide redox probe ( $\text{Fe}(\text{CN})_6^{3/4}$ ). As summarized in **Table 3**, SAMs of any appreciable chainlength on evaporated gold showed little or no  $\text{Fe}(\text{CN})_6^{3/4}$  redox activity (i.e., complete blocking behavior by the SAM indicated by the no peaks designation “NP” in Table 3). Indeed, only the MHOL SAM at evaporated gold exhibited small anodic and cathodic diffusional waves for  $\text{Fe}(\text{CN})_6^{3/4}$  while SAMs of BT and MHA at evaporated gold yielded only small anodic signals (indicated by “AN” in Table 3). On the other hand, all SAMs of significant chainlength formed on gold derived from the thermolysis of  $\text{Cu}^{2+}$  M-L MPC films revealed significant redox activity. **Figure 4** illustrates an example of this type of result comparison, showing  $\text{Fe}(\text{CN})_6^{3/4}$  voltammetry at a bare gold electrode, a DDT SAM on evaporated gold, and at DDT SAM on  $\text{Cu}^{2+}$  M-L MPC gold. From this result, it is clear that the DDT SAM formed on the NP gold (trace b in Figure 4) clearly allows redox probe ( $\text{Fe}(\text{CN})_6^{3/4}$ ) access to the electrode, another indication that these films have a high density of defects. Of the SAMs on  $\text{Cu}^{2+}$  M-L MPC gold showing voltammetry, the most significant blocking behavior recorded was with the carboxylic acid terminated films, MUA and MHDA. The apparent enhanced blocking ability of these films is most likely due to the combination of the longer chainlength of the SAMs and the electrostatic repulsion between the negatively charged carboxylic acid endgroups and anionic ferricyanide probe. Taken collectively, however, the redox probing results with  $\text{Fe}(\text{CN})_6^{3/4}$  are consistent with the capacitance and desorption results that suggest the SAMs on the NP-based gold possess a high density of defects.

As in other literature reports [30], a neutral ferrocene derivative called hydroxymethyl ferrocene (HMFc) was utilized as a more defect sensitive redox probe for the methyl terminated SAM systems. The higher hydrophobicity of HMFc, coupled with its ability to maintain

solubility in aqueous environments, allows for a greater propensity to interact with the SAM, thereby making it more sensitive to defects in the film [30]. In a similar fashion to  $\text{Fe}(\text{CN})_6^{3/4-}$ , the diffusional voltammetry of HMFC transitions from reversible to quasi-reversible with attenuated current flow or increases in the anodic and cathodic peak potentials ( $\Delta E_p$ ) as the SAM increases in chainlength and is more effective at blocking access to the electrode. SAMs with significant defect density, because of the nature of the HMFC, are likely to exhibit diffusional behavior closer to that of an unmodified gold interface (i.e., lower values of  $\Delta E_p$ ). HMFC probing of unfunctionalized SAMs on both types of substrates again revealed the same trend as seen with  $\text{Fe}(\text{CN})_6^{3/4-}$  with regard to the gold substrates. For example, voltammetry of HMFC at SAMs of BT, OT, and DDT on evaporated gold had an average  $\Delta E_p$  of 73, 101, and 253 mV, respectively. Identical films formed on the  $\text{Cu}^{2+}$  M-L MPC gold showed systemically lower average values of 60, 95, and 110 mV for  $\Delta E_p$ , respectively, indicating that these films possess defect density that allows more facile redox activity of HMFC.

All three electrochemical techniques for characterizing SAMs strongly suggest that, despite their identical physical appearance, there is a fundamental difference between the evaporated gold substrates and the thermolyzed M-L MPC films that directly contributes to a higher density of defects in SAMs on the latter substrate. X-ray photoelectron spectroscopy (XPS) of the unmodified gold substrates revealed that the substrates formed from thermolysis of the  $\text{Cu}^{2+}$ -linked MPC film possessed a significantly higher surface concentration of copper (average 3%) than the evaporated gold substrates (average 0.1%). Several reports indicate that this may be a source for defects in the SAM adlayers. Specifically, Guo [31] and Finklea [33] suggest that surface impurities such as copper deposits can serve as loci for defect sites in SAMs. Moreover, even though alkanethiols are known to spontaneously bond to copper metal, SAMs on copper

substrates have been found to have different properties than corresponding films on gold substrates, including significantly different structure (e.g., bond angle) [57]. If significant amounts of copper are deposited on a gold substrate, subsequent SAMs formed on those surfaces could display a mixture of properties typical to SAMs formed on uncompromised metal surfaces. The copper contamination is likely to produce SAMs with greater interfacial heterogeneity and regions of disorder, both of which could serve as sources for defects.

#### *4.2. Dependence of SAM Properties on MPC Film Assembly Strategy and Treatment*

##### *4.2.1. Low Metal Ion Exposure During MPC Film Assembly*

In order to examine if the source of SAM defect density on the thermolyzed gold films was related to the metal ion content of the MPC film precursor, alternative assembly procedures developed in our laboratory were employed to minimize the amount of excess metal ions within the MPC films [36]. The basis of the alternative assembly procedures was to limit the exposure of the MPC film to the metal ion linker solution. Well-established in the literature, a key aspect of the growth mechanism for these multi-layer MPC films is the mobility of the metal ions within the film that allow for the self-assembly of additional, multiple layers of MPC during a single, one hour exposure to MPCs [11,35]. In the alternative procedure, the extensive rinsing after exposure to metal linker or MPC solutions is unchanged but the metal exposure is limited to only one minute. As described elsewhere [36], this low metal exposure procedure produces films of equal thickness and identical properties compared to the traditional procedures [11,35] but should also limit excess (uncoordinated) metal ions within the film due to extensive rinsing and minimizing the penetration of the metal ions into the film during film growth (see Figure 5A,

inset). Essentially the procedure focuses the use of metal ions at the film-solution interface where they only serve to bind additional MPCs.

Within the collective results of this study, a very minor metal dependence trend is observable. That is, in comparing results from the  $\text{Cu}^{2+}$  M-L films with the  $\text{Zn}^{2+}$  M-L films (Supplementary Materials), SAMs on the latter substrates consistently exhibited slightly lower  $C_{dl}$  (Table SM-1), slightly more negative desorption potentials (Table SM-2), and increased blocking behavior toward the  $\text{Fe}(\text{CN})_6^{3-/4-}$  redox probe (Table SM-3). Even though  $\text{Cu}^{2+}$  linked MPC assemblies are very common in the literature [11,35], the aforementioned XPS results confirming copper contamination of the gold, as well as the well known ability of copper and gold to form alloys, motivated the use of zinc ions as another MPC linking system. Because  $\text{Zn}^{2+}$  is a weaker oxidizing agent than  $\text{Cu}^{2+}$ , Zn metal is less likely to co-deposit with the gold film. Thus, for this part of the study, a second alteration to our assembly strategy for the MPC films was the use of  $\text{Zn}^{2+}$  as opposed to  $\text{Cu}^{2+}$  metal ion linkers.  $\text{Zn}^{2+}$  M-L films were grown to similar thicknesses (as determined by optical absorbance measurements on the films) as the  $\text{Cu}^{2+}$  M-L films and thermolyzed before being modified with SAMs. After thermal treatment, the  $\text{Zn}^{2+}$  MPC gold substrates were immediately modified with methyl-terminated SAMs and subjected to the same electrochemical testing as before.

$C_{dl}$  measurements of the SAMs on the low exposure M-L  $\text{Zn}^{2+}$  MPC gold revealed a striking difference compared to the values recorded for the thermolyzed films from the traditionally assembled  $\text{Cu}^{2+}$  and  $\text{Zn}^{2+}$  M-L MPC films, especially when compared to the films on evaporated gold substrates as well (**Figure 5A**). As can be seen in the figure, methyl-terminated SAMs on the low exposure  $\text{Zn}^{2+}$  MPC gold display much lower capacitance, nearly matching that of the evaporated gold films. Likewise, **Figure 5B**, illustrates linear sweep desorption results for the

methyl-terminated SAMs that reinforce the phenomenon. SAMs on Cu<sup>2+</sup> MPC gold desorbed at much lower potentials than the same films on evaporated gold, but SAMs on Zn<sup>2+</sup> MPC gold formed with low exposure were found to desorb at similar potentials to the same SAMs on evaporated gold. This similarity was especially pronounced at longer chainlengths where structural order in the SAM is higher and more influenced by the nature of the gold substrate [32,33]. Results with redox probing analysis of these low exposure films were also consistent with the findings of the capacitance and desorption results. For example, Fe(CN)<sub>6</sub><sup>3/4-</sup> probing for defects at a DDT SAM on the low exposure Zn<sup>2+</sup> MPC gold resulted in voltammetry that was virtually indistinguishable from that of the evaporated gold (results not shown). More sensitive HMFC redox probing at methyl terminated SAMs on the low exposure Zn<sup>2+</sup> MPC gold reiterated the overall theme as well. **Figure 6** tracks the peak splitting ( $\Delta E_p$ ) of HMFC voltammetry at methyl terminated SAMs on the various types of gold and shows that for SAMs larger than BT, a substantially larger  $\Delta E_p$  value (i.e., fewer defects in the SAM) compared to Cu<sup>2+</sup> MPC gold, a result that is also more aligned with SAMs at evaporated gold. In fact, we note that similar peak splitting (~250 mV) of the HMFC voltammetry was recorded for an OT SAM at the low exposure Zn<sup>2+</sup> gold as at a DDT SAM at evaporated gold (comparing black arrows in Figure 6) even though the chainlengths differ by 4 methylene units. Results for low exposure M-L (Zn<sup>2+</sup>) films modified with DDT were not included as the probe was completely blocked (no peaks observed) and prevented a measurable  $\Delta E_p$  in that specific case.

#### 4.2.2. *Metal Ion Extraction from MPC Films Prior to Thermal Treatment*

To further the hypothesis regarding the important role of excess metal ions in MPC films that are to be thermally treated for use as a gold substrate for SAMs and to assess the degree to

which we have control over determining the defect density of SAMs on these surfaces, excess metal ions were extracted from the MPC films prior to thermolysis. Briefly, films of  $Zn^{2+}$  M-L films were grown with traditional 1 hour exposure to both  $Zn^{2+}$  solutions as well as the MPC solutions to ensure deep metal penetration into the film (Figure 5A, inset, bottom). After growth of the film was completed, the films were immersed in pure ethanol (EtOH) solutions for up to 45 minutes, with the EtOH solution renewed every 15 minutes during this time. Exposure to pure EtOH should serve to swell the film and leech excess, uncoordinated metals from the film while maintaining film integrity [11]. Capacitance scans show that there is a substantial decrease in charging current during the first 10 minutes as excess metal ion is extracted rather quickly. This effect quickly levels off as charging current measured after 20 minutes of soaking is not significantly different than the 10 minute measurement. It is believed that this change in  $C_{dl}$  is directly attributable to the loss of the uncoordinated metal ions since spectroscopic scans of the films before and after the extraction show very little change in the overall absorbance, indicating the film is of similar thickness after extraction, and no corresponding shift in the NP's characteristic surface plasmon band at 550 nm, an indication that the MPCs have not rearranged or experienced a significant change in interparticle distances (Supplementary Materials).

Metal ions ( $Zn^{2+}$ ) were extracted from the MPC films with pure EtOH as described above, subsequently treated thermally in the oven, and modified with a select number of SAMs as before. Specifically, SAMs of significant chainlength (e.g., DDT, MUA, MUD) were used exclusively in order to avoid some of the erratic behavior of short chain SAMs and because of their prominent use in bioanalytical chemistry (Section 4.3, below).  $C_{dl}$  measurements and linear sweep desorption were both used to again assess SAM defect density. **Figure 7** serves as an example focusing on DDT SAMs of the  $C_{dl}$  trends observed and clearly shows that the extraction



procedure, after only 20 minutes of soaking, produced a DDT SAM of similar quality to the films formed from low metal ion exposure during assembly. Likewise, the  $C_{dl}$  of DDT SAMs on gold produced from either the extraction or the low exposure procedures remains substantially lower than the same SAM formed traditionally ( $Zn^{2+}$  M-L films) with no strategic alteration to assembly procedures and/or specific pretreatment and approaches the  $C_{dl}$  of DDT SAMs on evaporated gold.  $C_{dl}$  and desorption results for additional SAMs on these substrates are compiled in **Table 4** for comparison and reiterate that the quality of SAMs on gold formed from the MPC films can be controlled by manipulating assembly procedures and minimizing metal ion content. Results for extraction procedures on SAMs of MHDA, a significantly longer chainlength SAM, on these substrates created from  $Zn^{2+}$  M-L films revealed similar trends in  $C_{dl}$  and LSV (Supplementary Materials).

$Fe(CN)_6^{3-/4-}$  redox probing experiments at SAMs formed on gold substrates from MPC films that were metal-extracted prior to thermolysis confirm drastic improvement in SAM defect density. All SAMs previously revealing diffusional  $Fe(CN)_6^{3-/4-}$  voltammetry at untreated M-L films (Table 3) showed no corresponding Faradaic activity (i.e., no peaks) at the same films formed on substrates formed after extraction of excess metal ions as part of their assembly pretreatment (results not shown). For example,  $Fe(CN)_6^{3-/4-}$  redox probing of MUD SAMS formed from MPC films assembled traditionally with  $Cu^{2+}$  linkages resulted in a diffusional voltammogram shape with both anodic and cathodic peaks ( $\Delta E_p = 131$  mV, Table 3) whereas the same system at metal extracted films results in no peaks for the redox probe (i.e., the probe is completely blocked by a lower defect density film) and is similar to probing results of the same SAM at evaporated gold.

Analogous metal ion extraction experiments on a limited number of SAMs (e.g., MUA) formed on thermolyzed  $\text{Cu}^{2+}$  M-L MPC assemblies resulting in similar trends, significantly lower  $C_{dl}$ , more negative desorption potentials, and greater blocking ability compared to their untreated (i.e., no metal extraction) counterparts (results not shown). The specific metal dependence, the difference between  $\text{Cu}^{2+}$  and  $\text{Zn}^{2+}$ , is very subtle, particularly when compared to the results of the same SAM at traditional evaporated gold. As will be discussed below, it appears that the mere presence of *any* excess metal ion, regardless of  $\text{Zn}^{2+}$  vs.  $\text{Cu}^{2+}$ , clearly overshadows any specific metal dependence and dictates the overall properties of the SAM formed on these substrates.

Our results strongly suggest that the presence of excess and residual uncoordinated metal ions within the MPC films that are thermally treated to produce gold films for SAM modification is a critical issue. MPC films can also be assembled with strategies not involving electrostatic metal ion linkages at all and thus use no metal at all. One such assembly method seen in the literature is the use of covalent interparticle bridges created from ester coupling reactions [37] or dithiol linkers [16,58]. In our own laboratory, these methods have been successful at assembling MPC films but clearly exhibit approximate layer-by-layer growth [16,37] rather than the multi-layer growth per exposure to MPC solution observed with metal-linked MPC films. Thus, due to the significant thickness of the MPC films in the application studied in this report, covalently assembled films display insufficient film growth in a reasonable amount of time and are not recommended. In our lab, a limited number of experiments involving the thermolysis of dithiol-linked MPC films (not shown) were consistent with the results presented in this paper – the production of gold films that support low defect SAMs.

#### *4.3. Implications for SAM Application – Protein Monolayer Electrochemistry*

The collective results of this study indicate that SAMs formed on nanoparticle-based gold will have density of defects dependent on how the MPC precursor film is assembled, a variable that can be easily controlled. This type of control is important for many applications of SAMs in bioanalytical chemistry. One common use of SAMs is as an interfacial layer for controlling surface adsorption of proteins and enzymes for biological electron transfer (ET) studies [59]. One such system that has enjoyed attention in this area is the adsorption of the ET protein cytochrome c (Cc) to a SAM terminated with carboxylic acid endgroups [60]. With an asymmetric distribution of charged amino acids, Cc is an ideally designed to electrostatically adsorb to anionic interfaces such as a carboxylic acid terminated SAM (**Figure 8, inset**). Here, we use Cc at carboxylic acid terminated SAMs as a model system to study adsorbate behavior at the SAM systems in this study and the impact the defect density attributable to the MPC film assembly procedures prior to thermal decomposition can have on this particular application.

Gold substrates formed from thermolyzed, traditionally grown M-L  $Zn^{2+}$  MPC films, either soaked for metal ion extraction or not, were modified with a MUA SAM and exposed to a solution of Cc. In addition, a MUA SAM was also formed on evaporated gold and exposed to the same protein solution. The cyclic voltammetry of Cc adsorbed to all of these SAMs are shown in **Figure 8** where it is clear that the SAM at the  $Zn^{2+}$  M-L MPC film exhibits a drastically larger background signal (i.e., charging current) consistent with a higher density of defects in the SAM interface. Without taking steps to remove excess metal ions, the MUA SAM is subject to greater defect density and lower signal-to-noise ratios (S/N) that may obscure or mask the actual protein voltammetry [2]. For the MUA SAMs on both the evaporated gold as well as the gold from  $Zn^{2+}$  M-L MPC films that were metal extracted with ethanol soaks, this ratio is improved and more defined voltammetry is observed.

#### 4. Conclusions

Films of MPCs can be assembled on glass substrates and subsequently thermolyzed to produce thin gold coatings. While this technique has proved successful for creating gold films on both flat and irregular shaped substrates [17], the use of these materials in a specific application was largely unexplored. In this report, we investigated the gold coatings created in this manner as a supporting substrate for SAMs. Electrochemical techniques were used to evaluate the defect density of SAMs at gold substrates made from the temperature induced decomposition of MPC films as compared to the same SAMs on common evaporated gold electrodes. This work establishes three important findings about the properties of these SAMs on this type of gold substrate. First, expected SAM trends regarding the effects of endgroups and chainlength are also observed with SAMs on the gold substrates derived from the MPC films. That is, longer chainlength alkanethiols and more hydrophobic endgroups yield more structured SAMs with better blocking characteristics, regardless of the type of gold substrate. Second, while the observed trends are consistent with other types of SAMs, films formed on gold from the thermal treatment of MPCs were recognized as having a substantially higher density of defects than corresponding films on evaporated gold. Lastly, control over the density of defects in these SAMs is dependent on the linking mechanism, assembly strategy, and pretreatment of the MPC film prior to the thermal decomposition to form the gold coating. Specifically, the density of defects of the eventual SAM on the gold is directly related to the content of metal ion linkers in the MPC film precursor. This work showed that the defect density of SAMs on the gold substrates created from NP films can have a significant impact in how those SAMs can be used or how they perform in a specific application like protein monolayer electrochemistry

where it can impact the signal-to-background of the voltammetry. By better understanding the properties of SAMs that form on the NP-based gold, one can begin to engineer these methods for application to three-dimensional or porous materials applications [61-62].

### **Acknowledgements**

We gratefully acknowledge the National Science Foundation (CHE-1401593), Henry Dreyfus Teacher-Scholar Award Program, and Virginia's Commonwealth Health Research Board for generously supporting this research. Student support was also provided by Richmond's School of Arts & Sciences Undergraduate Research Committee and the Department of Chemistry Puryear-Topham Fund. Likewise, we acknowledge significant contributions from other student researchers in the group including Nick Poulos, D.J. Tognarelli, Katey Reighard, Kris Gerig, Morgan Vargo, Anne Galyean, Michael Freeman, and Debbie Campbell-Rance. We also would like to thank Aaron Rothrock and Dr. Mark Schoenfisch of the University of North Carolina at Chapel Hill for performing XPS measurements on our materials and Dr. Robert Miller of the University of Richmond for his assistance in synthesizing MHA. Special thanks is given to Drs. Tammy Leopold, Rene Kanters, Diane Kellogg, and Will Case, as well as Russ Collins, Phil Joseph, Mandy Mallory, and LaMont Cheatham - all of whom make undergraduate research possible at the University of Richmond.

### **References**

[1] Brown KR, Fox AP, Natan M (1996) Morphology-Dependent Electrochemistry of Cytochrome *c* at Au Colloid-Modified SnO<sub>2</sub> Electrodes. *J Am Chem Soc* 118:1154-1157

- [2] Loftus AF, Reighard K, Kapourales S, Leopold MC (2008) Monolayer-Protected Nanoparticle Film Assemblies as Platforms for Controlling Interfacial and Adsorption Properties in Protein Monolayer Electrochemistry. *J Am Chem Soc* 130:1649-1661
- [3] Hicks JF, Zamborini FP, Murray RW (2002) Dynamics of Electron Transfers between Electrodes and Monolayers of Nanoparticles. *J Phys Chem B* 106:7751-7757
- [4] Kim Y, Johnson RC, Hupp JT (2001) Gold Nanoparticle-Based Sensing of “Spectroscopically Silent” Heavy Metal Ions. *Nano Letters* 1:165-167
- [5] Guihen E, Glennon JD, (2003) Nanoparticles in separation science - Recent developments. *Anal Lett* 36:3309-3336
- [6] Yang L, E. Guihen, Holmes JD, Loughran M, O'Sullivan GP, and Glennon JD (2005) Gold nanoparticle-modified etched capillaries for open-tubular capillary electrochromatography. *Anal Chem* 77:1840-1846
- [7] Gross GM, Nelson DA, Grate JW, Synovec RE (2003) Monolayer-protected gold nanoparticles as a stationary phase for open tubular gas chromatography. *Anal Chem* 75:4558-4564
- [8] Zellers ET, Cai Q (2002) Dual-chemiresistor GC detector employing layer-protected metal nanocluster interfaces. *Anal Chem* 74:3533-3539
- [9] Templeton AC, Wuelfing WP, Murray RW (2000) Monolayer protected cluster molecules. *Acc Chem Res* 33:27-36
- [10] Feldheim DI, Foss CA (eds) (2002) *Metal Nanoparticles – Synthesis, Characterization, and Applications*. Marcel Dekker, New York
- [11] Zamborini FP, Leopold MC, Hicks JF, Kulesza PJ, Malik, MA, Murray RW (2002) Electron hopping conductivity and vapor sensing properties of flexible network polymer films of metal nanoparticles. *J Am Chem Soc* 124:8958-8964
- [12] Evans SD, Johnson SR, Cheng YL, Shen T (2000) Vapour sensing using hybrid organic–inorganic nanostructured materials. *J Mater Chem* 10:183-188
- [13] Grate JW, Nelson DA, Skaggs R (2003) Sorptive behavior of monolayer-protected gold nanoparticle films: Implications for chemical vapor sensing. *Anal Chem* 75:1868-1879
- [14] H. Wohltjen and A. W. Snow, *Anal. Chem.* 70 (1998) Colloidal metal-insulator-metal ensemble chemiresistor sensor. 2856-2859
- [15] Han L, Daniel DR, Maye MM, Zhong C (2001) Core-shell nanostructured nanoparticle films as chemically sensitive interfaces. *Anal Chem* 73:4441-4449

- [16] Russell LE, Pompano RR, Kittredge KW, and Leopold MC (2007) Assembled nanoparticle films with crown ether-metal ion "sandwiches" as sensing mechanisms for metal ions. *J Mater Sci* 42:7100-7108
- [17] Wuelfing WP, Zamborini FP, Templeton AC, Wen X, Yoon H, Murray RW (2001) Monolayer-protected clusters: Molecular precursors to metal films. *Chem Mater* 13:87-95
- [18] Musick MD, Keating CD, Lyon LA, Botsko SL, Pena DJ, Holliway WD, McEvoy TM, Richardson JN, Natan MJ (2000) Metal films prepared by stepwise assembly. 2. Construction and characterization of colloidal Au and Ag multilayers. *Chem Mater* 12:2869-2881
- [19] Supriya L, Claus RO (2005) Colloidal Au/linker molecule multilayer films: Low-temperature thermal coalescence and resistance changes. *Chem Mater* 17:4325-4334
- [20] Yang N, Aoki K, Nagasawa H (2004) Thermal metallization of silver stearate-coated nanoparticles owing to the destruction of the shell structure. *J Phys Chem B* 108:15027-15032
- [21] Jiang P, Cizeron J, Bertone JF, Colvin VL (1999) Preparation of macroporous metal films from colloidal crystals. *J Am Chem Soc* 121:7957-7958
- [22] Luo L, Maye MM, Han L, Kariuki NN, Jones VW, Lin Y, Engelhard MH, Zhong C (2004) Spectroscopic characterizations of molecularly linked gold nanoparticle assemblies upon thermal treatment. *Langmuir* 20:4254-4260
- [23] Taniguchi I, Toyosawa K, Yamaguchi H, Yasukouchi K (1982) Reversible electrochemical reduction and oxidation of cytochrome-c at a bis(4-pyridyl) disulfide-modified gold electrode. *J Chem Soc Chem Comm* 1032-1033
- [24] Norman AG, Olson JM, Geisz JF, Moutinho HR, Mason A, Al-Jassim MM, Vernon SM (1999) Ge-related faceting and segregation during the growth of metastable (GaAs)<sub>(1-x)</sub>(Ge)<sub>2</sub>(x) alloy layers by metal-organic vapor-phase epitaxy. *Appl Phys Lett* 74:1382-1384
- [25] Fan FF, Yang J, Dirk SM, Price DW, Kosynkin D, Tour JM, Bard AJ (2001) Determination of the molecular electrical properties of self-assembled monolayers of compounds of interest in molecular electronics. *J Am Chem Soc* 123:2454-2455
- [26] Zamborini FP, Crooks RM (1998) Corrosion passivation of gold by n-alkanethiol self-assembled monolayers: Effect of chain length and end group. *Langmuir* 14:3279-3286
- [27] Gooding JJ, Mearns F, Yang W, Liu J (2003) Self-assembled monolayers into the 21(st) century: Recent advances and applications. *Electroanalysis* 15:81-96
- [28] Ulman A (1996) Formation and structure of self-assembled monolayers. *Chem Rev* 96:1533-1554

- [29] Meyers RA (ed.) (2010) Encyclopedia of Analytical Chemistry. John Wiley & Sons, New York, p 1-26
- [30] Creager SE, Hockett LA, Rowe GK (1992) Consequences of microscopic surface-roughness for molecular self-assembly. *Langmuir* 8:854-861
- [31] Guo L, Facci JS, McLendon G, Mosher R (1994) Effect of gold topography and surface pretreatment on the self-assembly of alkanethiol monolayers. *Langmuir* 10:4588-4593
- [32] Leopold MC, Black JA, Bowden EF (2002) Influence of gold topography on carboxylic acid terminated self-assembled monolayers. *Langmuir* 18:978-980
- [33] Finklea HO (1996) Electrochemistry of organized monolayers of thiols and related molecules on electrodes. *Electroanalytical Chemistry* 19:109-335
- [34] Nahir TM, Bowden EF (1996) The distribution of standard rate constants for electron transfer between thiol-modified gold electrodes and adsorbed cytochrome c. *J Electroanal Chem* 410:9-13
- [35] Zamborini FP, Hicks JF, Murray RW (2000) Quantized double layer charging of nanoparticle films assembled using carboxylate/(Cu<sup>2+</sup> or Zn<sup>2+</sup>)/carboxylate bridges. *J Am Chem Soc* 122:4514-4515
- [36] Sheibley D, Tognarelli DJ, Szymanik R, Leopold MC (2005) Ultra-fast formation and characterization of stable nanoparticle film assemblies. *J Mater Chem* 15:491-498
- [37] Tognarelli DJ, Miller RB, Pompano RR, Loftus AF, Sheibley DJ, Leopold MC (2005) Covalently networked monolayer-protected nanoparticle films. *Langmuir* 21:11119-11127
- [38] Goss CA, Charych DH, Majda M (1991) Application of (3-Mercaptopropyl)Trimethoxysilane as a molecular adhesive in the fabrication of vapor-deposited gold electrodes on glass substrates. *Anal Chem* 63:85-88
- [39] Brust M, Fink J, Bethell D, Schiffrin DJ, Kiely C (1995) Synthesis and reactions of functionalized gold nanoparticles. *J Chem Soc Chem Comm* 1655-1656
- [40] Hicks JF, Miles DT, Murray RW (2002) Quantized double-layer charging of highly monodisperse metal nanoparticles. *J Am Chem Soc* 124:13322-13328
- [41] Ingram RS, Hostetler MJ, Murray RW (1997) Poly-hetero-omega-functionalized alkanethiolate-stabilized gold cluster compounds. *J Am Chem Soc* 119:9175-9178
- [42] Templeton AC, Hostetler MJ, Warmoth EK, Chen S, Hartshorn CM, Krishnamurthy VM, Forbes MDE, Murray RW (1998) Gateway reactions to diverse, polyfunctional monolayer-protected gold clusters. *J Am Chem Soc* 120:4845-4849



[43] Baker LA, Zamborini FP, Sun L, Crooks RM (1999) Dendrimer-mediated adhesion between vapor-deposited Au and glass or Si wafers. *Anal Chem* 71:4403-4406

[44] As in other reports, films assembled with zinc ions serving as the linking bridge required the deprotonation of the MPC's carboxylic acid functional groups by adjusting the basicity of the metal ion dipping solution with the addition of 10-50  $\mu$ L of 1 mM KOH to the 10 mL vial

[45] Greenwood NN, Earnshaw A (1984) *Chemistry of the Elements*. Pergamon Press, New York

[46] MHA was not available commercially at reasonable prices and had to be synthesized according to the procedure described in the Supplementary Materials

[47] Bard AJ, Faulkner LR (1980) *Electrochemical Methods Fundamentals and Applications*. John Wiley & Sons, New York

[48] Since this study is focused on the general assessment of overall SAM quality, we make no differentiation between pinhole defects, where solvent is able to contact gold, and point defects in the SAM, where the gold is not exposed but solvent can approach the electrode closer than the average thickness of the SAM. We use the term "defect density" to describe both types of defects [33]

[49] Miller C, Cuendet P, Graetzel M (1991) Adsorbed omega-hydroxy thiol monolayers on gold electrodes – evidence for electron-tunneling to redox species in solution. *J Phys Chem* 95:877-886

[50] Kielland J (1937) Individual Activity Coefficients of Ions in Aqueous Solutions. *J Am Chem Soc* 59:1675-1678

[51] Weisshaar DE, Walczak MM, Porter MD (1993) Electrochemically induced transformations of monolayers formed by self-assembly of mercaptoethanol at gold. *Langmuir* 9:323-329

[52] Walczak MM, Popenoe DD, Deinhammer RS, Lamp BD, Chung C, Porter MD (1991) Reductive desorption of alkanethiolate monolayers at gold - a measure of surface coverage. *Langmuir* 7:2687-2693

[53] H. O. Finklea, S. Avery, M. Lynch and T. Furtch, *Langmuir* 3 (1987) Blocking oriented monolayers of alkyl mercaptans on gold electrodes. 409-413.

[54] Finklea HO, Snider DA, Fedyk J, Sabatani E, Gafni Y, Rubinstein I (1993) Characterization of octadecanethiol-coated gold electrodes as microarray electrodes by cyclic voltammetry and ac-impedance spectroscopy. *Langmuir* 9:3660-3667

[55] Chidsey CED, Bertozzi CR, Putvinski TM, Majsce AM (1990) Coadsorption of ferrocene-terminated and unsubstituted alkanethiols on gold - electroactive self-assembled monolayers. *J Am Chem Soc* 112:4301-4306

- [56] Groat KA, Creager SE (1993) Self-assembled monolayers in organic-solvents - electrochemistry at alkanethiolate-coated gold in propylene carbonate. *Langmuir* 9:3668-3675
- [57] Jennings GW, Laibinis PE (1997) Self-assembled n-alkanethiolate monolayers on underpotentially deposited adlayers of silver and copper on gold. *J Am Chem Soc* 119:5208-5214
- [58] Leibowitz FL, Zheng W, Maye MM, Zhong C (1999) Structures and properties of nanoparticle thin films formed via a one-step - Exchange-cross-linking - Precipitation route. *Anal Chem* 71:5076-5083
- [59] Prime KL, Whitesides GM (1991) Self-assembled organic monolayers – model systems for studying adsorption of proteins at surfaces. *Science* 252:1164-1167
- [60] Bowden EF (1997) Wiring Mother Nature: Interfacial Electrochemistry of Proteins. *Electrochemical Society Interface* 6:40-44
- [61] Wallace JM, Dening BM, Eden KB, Stroud RM, Long JW, Rolison DR (2004) Silver-colloid-nucleated cytochrome c superstructures encapsulated in silica nanoarchitectures. *Langmuir* 20:9276-9281
- [62] Wallace JM, Rice JK, Pietron JJ, Stroud RM, Long JW, Rolison DR (2003) Silica nanoarchitectures incorporating self-organized protein superstructures with gas-phase bioactivity. *Nano Letters* 3:1463-1467

## Captions

**Fig. 1.** Cyclic voltammetry for  $C_{60}$  measurements of DDT SAMs at gold substrates formed from the thermal decomposition of (a)  $Zn^{2+}$  M-L MPC films, (b)  $Cu^{2+}$  M-L MPC films, and (c) evaporated gold. **Inset:** Cyclic voltammetry of methyl-terminated alkanethiolate SAMs of varying chainlength on evaporated gold substrates in 1.0 M KCl. Current was measured at 250 mV (inset, dashed vertical arrow)

for  $C_{dl}$  calculations. Note: BT = butanethiolate SAM, OT = octanethiolate SAM, and DDT = dodecanethiolate SAM.

**Fig. 2.**  $C_{dl}$  trends of SAMs with varying endgroups and chainlength (n) on evaporated gold (closed symbols/solid trend lines) and  $Cu^{2+}$  M-L MPC gold substrates (open symbols – dotted trend lines) in 1.0 M KCl. **Inset:** Expansion of  $C_{dl}$  trends for SAMs on evaporated gold substrates (closed symbols)\*. Analogous results were observed with  $Zn^{2+}$  M-L MPC gold substrates and in different electrolytes (see Supplementary Materials).

**Fig. 3.** **A)** Examples of linear sweep voltammograms for the reductive desorption of methyl terminated DDT SAMs on (a)  $Cu^{2+}$  M-L MPC gold and (b) evaporated gold substrates in 1 M KOH solution. **B)** Reductive desorption peak potentials ( $E_p$ ) for methyl terminated SAMs of varying chainlength (n) on evaporated gold (closed symbols) and  $Cu^{2+}$  M-L MPC gold (open symbols) substrates.

**Fig. 4.** Cyclic voltammetry of 2 mM  $K_3Fe(CN)_6$  redox probe at (a) bare evaporated gold, (b) DDT SAM on  $Cu^{2+}$  M-L MPC gold, and (c) DDT SAM on evaporated gold. **Inset:** Expansion of voltammetry at DDT SAM on evaporated gold (c) showing complete blocking behavior.

**Fig. 5.** **A)**  $C_{dl}$  trends of methyl terminated SAMs of varying chainlength (n) on evaporated gold ( $\blacklozenge$ ) compared to M-L MPC gold (open symbols) where the MPC film was assembled with  $Cu^{2+}$  linkers ( $\Delta$ ) and  $Zn^{2+}$  linkers with either traditional procedures ( $\circ$ ) or with low exposure to  $Zn^{2+}$  ( $\square$ ) during MPC film assembly. **Inset:** Schematic representation of limiting metal ion penetration into the MPC film during assembly. Lowering exposure to metal ion species during this process (bottom) reduces the defect density in SAMs on gold substrates formed from these films. **B)** Reductive desorption peak potentials ( $E_p$ ) for methyl terminated SAMs of varying chainlength (n) on evaporated gold ( $\blacklozenge$ ),  $Cu^{2+}$  M-L MPC gold ( $\Delta$ ), and low exposure  $Zn^{2+}$  M-L MPC gold ( $\square$ ).

**Fig. 6.** Peak potential difference ( $\Delta E_p$ ) between anodic ( $E_{pa}$ ) and cathodic ( $E_{pc}$ ) peak potentials of HMFc redox probe cyclic voltammetry at SAMs of varying chainlength (n) on evaporated gold ( $\blacklozenge$ ), M-L  $Cu^{2+}$  MPC gold ( $\Delta$ ), and M-L  $Zn^{2+}$  MPC gold assembled with low exposure to  $Zn^{2+}$  ( $\square$ ). The black arrows illustrate a dramatic comparison in that the  $\Delta E_p$  for HMFc at an OT SAM on gold formed from the thermolysis of a  $Zn^{2+}$  M-L MPC film is similar ( $\sim 250$  mV) compared to a significantly longer DDT SAM at evaporated gold.

**Fig. 7.** Cyclic voltammetry for  $C_{dl}$  measurements of DDT SAMs at gold substrates formed from the thermal decomposition of (a)  $Zn^{2+}$  M-L MPC films, (b)  $Zn^{2+}$  M-L MPC films with low exposure to  $Zn^{2+}$  during assembly, (c)  $Zn^{2+}$  M-L MPC films that were soaked or metal extracted with ethanol after assembly/prior to thermal decomposition and (d) evaporated gold.

**Fig. 8.** Protein monolayer electrochemistry or cyclic voltammetry of cytochrome c at MUA SAMs on (a)  $Zn^{2+}$  M-L MPC films, (b)  $Zn^{2+}$  M-L MPC films that were soaked (metal extracted) with ethanol after assembly/prior to thermal decomposition and (c) evaporated gold.